

Binding and Electron Transfer between Cytochrome b_5 and the Hemoglobin α - and β -Subunits through the Use of [Zn, Fe] Hybrids

Naomi R. Naito, He Huang, Annie Willie Sturgess, Judith M. Nocek, and Brian M. Hoffman*

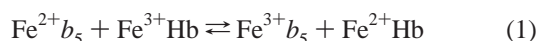
Contribution from the Department of Chemistry, Northwestern University, 2145 Sheridan Road, Evanston, Illinois 60208

Received June 8, 1998

Abstract: We have measured the binding affinity (K_A) and electron transfer (ET) rate constants (k) for the complex of hemoglobin (Hb) and cytochrome b_5 (b_5), using triplet quenching titrations of mixed-metal [ZnM, $\text{Fe}^{3+}(\text{N}_3^-)$] Hb hybrids and of fully substituted Zn–mesoporphyrin (ZnM)Hb by b_5 (trypsin-solubilized, bovine) (pH values 6.0 and 7.0). The use of the mixed-metal Hb hybrids with Zn in one chain type allows us to selectively monitor the $^3\text{ZnP} \rightarrow \text{Fe}^{3+}\text{P}$ ET reaction of $\text{Fe}^{3+}b_5$ with either the α -chains or the β -chains. The self-consistent analysis of the results for the mixed-metal hybrids and those for the (ZnM)Hb allows us to determine the reactivity and affinity constants for the interactions of b_5 with the individual subunits of T-state Hb. The results confirm that ET occurs within a complex between b_5 and Hb, not through a simple bimolecular collision process. At pH 6.0, the binding affinity constant of the α -chains ($K_\alpha \approx 2.0 \times 10^4 \text{ M}^{-1}$) is ~ 4 -fold larger than that of the β -chains ($K_\beta = 4.9 \times 10^3 \text{ M}^{-1}$); the intracomplex ET rate constant of the α -chains ($k_\alpha \approx 1500 \text{ s}^{-1}$) is ~ 2 -fold larger than that of the β -chains ($k_\beta \approx 850 \text{ s}^{-1}$). The binding affinity and ET rate constant of the α -chains both decrease as the pH is increased from 6.0 to 7.0; the binding affinity of the β -chains is essentially the same at pH 6.0 and 7.0, while the ET reactivity decreases. The kinetic results are consistent with a docking model in which each subunit binds a molecule of b_5 . However, they permit an alternative in which b_5 reacts with the α -chains by binding at a site which spans the $\alpha_1\beta_2$ dimer interface.

Introduction

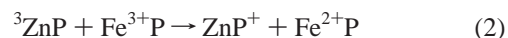
Ferrous hemoglobin (Fe^{2+}Hb) functions in oxygen transport, but under physiological conditions, both oxyHb and deoxyHb can be oxidized to inactive metHb (Fe^{3+}Hb). In the erythrocyte, the concentration of Fe^{3+}Hb is maintained at a low level by an electron-transport chain in which a soluble cytochrome b_5 (b_5) mediates electron transfer between the flavin-containing cytochrome b_5 reductase and Fe^{3+}Hb .^{1–3} In this paper, we focus on the terminal electron-transfer (ET) step, in which $\text{Fe}^{2+}b_5$ is the electron donor to Fe^{3+}Hb (eq 1).



This reaction appears to involve the formation of an electrostatic protein–protein complex between Fe^{3+}Hb and $\text{Fe}^{2+}b_5$ in which one molecule of b_5 binds to each subunit of the $\alpha_2\beta_2$ Hb tetramer. Isoelectric focusing experiments were used to qualitatively detect the formation of a protein–protein complex.⁴ Subsequently, Mauk and co-workers^{5,6} reported that the interaction of b_5 with Hb gives rise to a perturbation in the optical spectrum, and used this change to quantitatively characterize the binding between these two proteins. These studies showed

that the binding of b_5 to Hb depends on both ionic strength and pH, indicating that electrostatic interactions stabilize this ET complex. In contrast, McLendon and co-workers recently suggested that prior complex formation may not be necessary for ET between these partners.⁷

Substitution of the heme (FeP) of one partner of an ET complex by a closed-shell metalloporphyrin (MP), $\text{M} = \text{Zn}$ (or Mg), offers a means of studying binding and intracomplex ET.^{8–11} The triplet state, ^3ZnP , produced by laser-flash excitation is a strong reductant, and in the presence of a quencher (Fe^{3+}P), its lifetime is decreased by long-range, intracomplex $^3\text{ZnP} \rightarrow \text{Fe}^{3+}\text{P}$ ET (eq 2). The resulting ET intermediate (**I**)



returns to the ground state by the thermally activated ET from the Fe^{2+}P to the porphyrin-center π -cation radical, ZnP^+ , according to (eq 3). This metal-substitution approach has been



applied to the [Hb, b_5] complex,^{12–14} as well as to the related

(1) Hultquist, D. E.; Passon, P. G. *Nature (London) New Biol.* **1971**, *229*, 252–254.

(2) Sannes, L. J.; Hultquist, D. E. *Biochim. Biophys. Acta* **1978**, *544*, 547–554.

(3) Abe, K.; Sugita, Y. *Eur. J. Biochem.* **1979**, *101*, 423–428.

(4) Righetti, P. G.; Gacon, G.; Gianazza, E.; Lostanlen, D.; Kaplan, J.-C. *Biochem. Biophys. Res. Commun.* **1978**, *85*, 1575–1581.

(5) Mauk, M. R.; Mauk, A. G. *Biochemistry* **1982**, *21*, 4730–4734.

(6) Mauk, M. R.; Reid, L. S.; Mauk, A. G. *Biochem. J.* **1984**, *221*, 297–302.

(7) Qiao, T.; Witkowski, R.; Henderson, R.; McLendon, G. *JBIC* **1996**, *1*, 432–438.

(8) Nocek, J. M.; Zhou, J. S.; De Forest, S.; Priyadarshy, S.; Beratan, D. N.; Onuchic, J. N.; Hoffman, B. M. *Chem. Rev.* **1996**, *96*, 2459–2489.

(9) McLendon, G.; Hake, R. *Chem. Rev.* **1992**, *92*, 481–490.

(10) Hoffman, B. M.; Natan, M. J.; Nocek, J. M.; Wallin, S. A. *Struct. Bond.* **1991**, *75*, 85–108.

(11) Kostic, N. M. *Metal Ions Biol. Syst.* **1991**, *27*, 129–182.

(12) Simmons, J.; McLendon, G.; Qiao, T. *J. Am. Chem. Soc.* **1993**, *115*, 4889–4890.

(13) Qiao, T.; Simmons, J.; Horn, D. A.; Chandler, R.; McLendon, G. *J. Phys. Chem.* **1993**, *97*, 13089–13091.

[Mb, b_5] complex.^{15,16} McLendon and co-workers reported the rapid reduction of $\text{Fe}^{3+}b_5$ by intracomplex ET (eq 2) ($k_{\text{et}} \approx 8000 \text{ s}^{-1}$) when $\text{Fe}^{3+}b_5$ is bound at the α -chain of the $[\alpha\text{ZnP}, \beta\text{Fe}^{3+}(\text{CN}^-)]$ hybrid at low ionic strength.¹⁴ Although similar experiments with the complementary $[\alpha\text{Fe}^{3+}(\text{CN}^-), \beta\text{ZnP}]$ hybrid were not performed, McLendon and co-workers¹³ later reported that the triplet decay traces obtained when ZnHb is quenched with $\text{Fe}^{3+}b_5$ were biphasic ($k_1 = 2700 \text{ s}^{-1}$ and $k_2 = 310 \text{ s}^{-1}$). No explanation was offered for the biphasic kinetic results, but clearly the two phases could not self-consistently correspond to quenching at the individual subunits, because neither rate constant corresponds to that reported for the $[\alpha\text{ZnP}, \beta\text{Fe}^{3+}(\text{CN}^-)]$ hybrid.

In the present report, we use the $\text{Fe}^{3+}b_5$ triplet quenching of both subunits within ZnHb and of either the αZn or the βZn subunit in the mixed-metal $[\text{Zn}, \text{Fe}^{3+}]$ Hb hybrids to measure the binding and ET rate constants for the reaction between $\text{Fe}^{3+}b_5$ and T-state Hbs (eq 2). Experiments with the hybrids selectively monitor the reaction of a single chain type with $\text{Fe}^{3+}b_5$ whereas experiments with fully substituted ZnHb monitor the superposition of the independent reactions occurring at each chain. We *self-consistently* interpret these results to determine the individual binding and quenching constants for the α - and the β -chains within T-state Hb. The kinetic measurements are consistent with a docking model in which each subunit binds a molecule of b_5 ,¹⁷ but our results and variant studies¹⁸ also permit an alternate model in which b_5 reacts with the α -chains by binding at a site which spans the $\alpha_1\beta_2$ dimer interface.

Experimental Procedures

Materials. HbA₀ was isolated from out-dated whole blood as previously described.^{19,20} The trypsin-solubilized bovine cytochrome b_5 was prepared according to the method of Mauk and co-workers.²¹ Zn mesoporphyrin IX (ZnM) was purchased from Porphyrin Products (Logan, UT). D-Glucose, glucose oxidase (type x-5 from *Aspergillus niger*), and bovine liver catalase (thymol free) were purchased from Sigma. The *p*-hydroxymercuribenzoic acid (PMB) and inositol hexaphosphoric acid (IHP) were purchased from Sigma as the sodium salts. The β -mercaptoethanol (BME) was purchased from Aldrich. Atomic absorption standards were purchased from Mallinckrodt.

Isolation of (ZnM)Hb and [ZnM, FeP] Hybrids. We employed Zn mesoporphyrin (ZnM), rather than Zn protoporphyrin for spectroscopic reasons presented in the Results. (ZnM)Hb was prepared as published.²⁰ The chain method of Yip and co-workers²² was used to make the $[\alpha\text{ZnM}, \beta\text{Fe}^{2+}(\text{CO})]$ hybrid. Hb was allowed to react with PMB, and the $\alpha\text{Fe}^{2+}(\text{CO})$ -PMB and $\beta\text{Fe}^{2+}(\text{CO})$ -PMB₂ chains were separated on an anion exchange (DE-52) column and then reacted with β -mercaptoethanol (BME) to remove the PMB. Heme-free α -chains were prepared and then reconstituted with ZnM. These αZnM chains were recombined with $\beta\text{Fe}^{2+}(\text{CO})$ chains to form the $[\alpha\text{ZnM}, \beta\text{Fe}^{2+}(\text{CO})]$ hybrid. The βZnM chains are difficult to make directly by the reconstitution of apo β -chains so we tried the semi-globin method to make the β -hybrid. The apo β -chains were recombined with $\alpha\text{Fe}^{2+}(\text{CO})$ chains to form semi-globin, and then ZnM was added. However, the β -hybrids made by this method are nonhomogeneous and occur in

poor yields because the ZnM tends to replace the heme in the α -chains in the reconstitution step, rather than incorporating into the apo β -chains. To avoid this heme exchange, we made βZnM chains from (ZnM)Hb. (ZnM)Hb was prepared and reacted with PMB, and the ZnM-PMB-chains were separated on an anion exchange (DE-52) column. The isolated βZnM -PMB₂ chains were reacted with BME to regenerate the βZnM chains which were recombined with $\alpha\text{Fe}^{2+}(\text{CO})$ chains to form the $[\alpha\text{Fe}^{2+}(\text{CO}), \beta\text{ZnM}]$ hybrid with a yield of about 30%.

The $[\alpha\text{ZnM}, \beta\text{Fe}^{2+}(\text{CO})]$ hybrid, $[\alpha\text{Fe}^{2+}(\text{CO}), \beta\text{ZnM}]$ hybrid, and (ZnM)Hb were further purified by HPLC (Waters 650). The recombination mixture was loaded onto a TSK-based cation exchange column (Beckman, 21.5 mm \times 15 cm, SP-5PW) that had been preequilibrated with 25 mM potassium phosphate (KPi) buffer at pH 6.0 and was eluted with a two-step linear gradient. The first step was a 5 min linear gradient from the equilibration buffer to 40% 25 mM K_2HPO_4 , and the second step was a 75 min linear gradient to 25 mM K_2HPO_4 , at a flow rate of 5 mL/min. The absorbance was monitored at 280, 414, and 576 nm (Waters 490 D multichannel detector). The isolated hybrids and (ZnM)Hb were homogeneous by isoelectric focusing and were stored in liquid nitrogen.

The kinetic measurements of the ET reaction between the individual ZnM chains and b_5 employed the $[\text{ZnM}, \text{Fe}^{3+}(\text{N}_3^-)]$ hybrids. The N_3^- ligand was used on the ferric chain because previous studies with $[\text{ZnP}, \text{Fe}^{3+}(\text{L})]$ hybrids showed that the intratetramer ET reaction between a ZnP subunit and a ferric subunit is slow for anionic ligands.¹⁰ Thus, the intratetramer reaction does not compete with the intermolecular ET reaction between the Hb subunits and b_5 . Of the anionic ligands available (N_3^- , CN^- , F^-), N_3^- is the best for the pH range of 6.0–7.0 because F^- binds much more weakly and CN^- has a pK_a of 9.31. The $[\text{ZnM}, \text{Fe}^{2+}(\text{CO})]$ hybrids were oxidized with $\text{K}_3\text{Fe}(\text{CN})_6$ in 50 mM KPi, pH 6.0, buffer at 4 °C under nitrogen atmosphere. Excess NaN_3 was added as the ligand to the Fe^{3+} chains. The excess oxidant was removed by gel filtration using Sephadex G-25 (fine, Sigma) columns. The $[\text{ZnM}, \text{Fe}^{3+}(\text{N}_3^-)]$ hybrids were exchanged into 5 mM KPi, 5 mM NaN_3 , 0.05 mM IHP buffer using Centricon-10 microconcentrators (Amicon). Anaerobic samples for the kinetic measurements were prepared in Pyrex cuvettes containing 2 mL of nitrogen-purged 5 mM KPi, 5 mM NaN_3 , 0.05 mM IHP buffer. CO-recombination studies with $[\text{ZnP}, \text{Fe}^{2+}(\text{CO})]$ hybrids show that, in the presence of IHP, the hybrids can be quantitatively converted to the T-state conformation.²³ The oxygen scavenging system of 5 mM D-glucose, 25 $\mu\text{g}/\text{mL}$ thymol-free catalase from bovine liver, and 100 $\mu\text{g}/\text{mL}$ glucose oxidase was used.²⁴ Hybrid concentrations were typically about 4 μM in subunits. For the titrations, aliquots of a $\sim 1 \text{ mM}$ stock solution of $\text{Fe}^{3+}b_5$ ($\epsilon_{413} = 117 \text{ mM}^{-1} \text{ cm}^{-1}$)²⁵ were added to the hybrid solution. The protein stock solutions were deaerated with nitrogen prior to addition to the sample.

The subunit concentrations for the hybrids were determined from the extinction coefficients obtained from simulated spectra derived from the spectra of the parent species. For the $[\text{ZnM}, \text{Fe}^{2+}(\text{CO})]$ hybrid spectrum, the spectrum of (ZnM)Hb, normalized to the value at the Soret ($\epsilon_{414} = 360 \text{ mM}^{-1} \text{ cm}^{-1}$; ICP-AES Thermo Jarrell Ash Atomscan 25), was added to the spectrum of $\text{Fe}^{2+}(\text{CO})\text{Hb}$, normalized to the value at the Soret ($\epsilon_{418} = 208 \text{ mM}^{-1} \text{ cm}^{-1}$),²⁶ and the resulting spectrum was divided by 2 to generate extinction coefficients per subunit. This simulated $[\text{ZnM}, \text{Fe}^{2+}(\text{CO})]$ hybrid spectrum has a Soret maximum at 414 nm with $\epsilon_{414} = 267 \text{ mM}^{-1} \text{ cm}^{-1}$. For the $[\text{ZnM}, \text{Fe}^{3+}(\text{N}_3^-)]$ hybrid spectrum, the normalized (ZnM)Hb spectrum was averaged with the spectrum of $\text{Fe}^{3+}(\text{N}_3^-)\text{Hb}$, normalized to the value at the Soret maximum ($\epsilon_{418} = 118 \text{ mM}^{-1} \text{ cm}^{-1}$).²⁷ This simulated $[\text{ZnM}, \text{Fe}^{3+}(\text{N}_3^-)]$ hybrid spectrum has a Soret at 414 nm with $\epsilon_{414} = 234 \text{ mM}^{-1} \text{ cm}^{-1}$.

Laser-Flash Photolysis. Photoexcitation was achieved with a Q-switched, frequency-doubled Nd:YAG YG660A laser (Continuum,

(14) Simolo, K. P.; McLendon, G. L.; Mauk, M. R.; Mauk, A. G. *J. Am. Chem. Soc.* **1984**, *106*, 5012–5013.

(15) Nocek, J. M.; Sishta, B. P.; Cameron, J. C.; Mauk, A. G.; Hoffman, B. M. *J. Am. Chem. Soc.* **1997**, *119*, 2146–2155.

(16) Jiang, M.; Ning, Q.; Hoffman, B. M. *Biochemistry*, submitted.

(17) Poulos, T. L.; Mauk, A. G. *J. Biol. Chem.* **1983**, *258*, 7369–7373.

(18) Gacon, G.; Losten, D.; Labie, D.; Kaplan, J.-C. *Proc. Natl. Acad. Sci. U.S.A.* **1980**, *77*, 1917–1921.

(19) Williams, R. C.; Tsay, K. *Anal. Biochem.* **1973**, *54*, 137–145.

(20) Scholler, D. M.; Wang, M.-Y. R.; Hoffman, B. M. *Methods Enzymol.* **1978**, *52C*, 487–493.

(21) Reid, L. S.; Mauk, A. G. *J. Am. Chem. Soc.* **1982**, *104*, 841–845.

(22) Yip, Y. K.; Waks, M.; Beychok, S. *Proc. Natl. Acad. Sci. U.S.A.* **1977**, *74*, 64–68.

(23) Blough, N. V.; Zemel, H.; Hoffman, B. M.; Lee, T. C. K.; Gibson, Q. H. *J. Am. Chem. Soc.* **1980**, *102*, 5683–5685.

(24) Stankovich, M. T.; Schopfer, L. M.; Massey, V. *J. Biol. Chem.* **1978**, *253*, 4971–4979.

(25) Ozols, J.; Strittmatter, P. *J. Biol. Chem.* **1964**, *239*, 1018–1023.

(26) Banerjee, R.; Alpert, Y.; Leterrier, F.; Williams, R. J. P. *Biochemistry* **1969**, *8*, 2862–2867.

(27) Perutz, M. F.; Heidner, E. J.; Ladner, J. E.; Beestone, J. G.; Ho, C.; Slade, E. F. *Biochemistry* **1974**, *13*, 22187–2200.

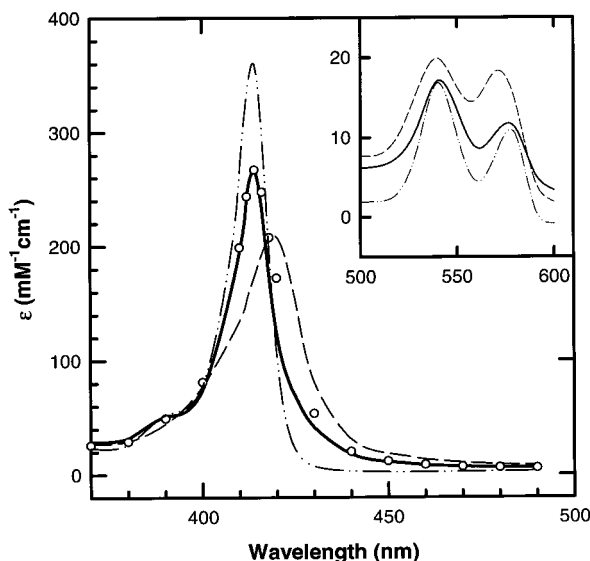


Figure 1. Absorption spectra of $\text{Fe}^{2+}(\text{CO})\text{Hb}$ (---), $(\text{ZnM})\text{Hb}$ (- · - ·), $[\alpha\text{ZnM}, \beta\text{Fe}^{2+}(\text{CO})]$ hybrid (—), and simulated $[\alpha\text{ZnM}, \beta\text{Fe}^{2+}(\text{CO})]$ hybrid (○). Conditions: 10 mM KPI, pH 7.0, 20 °C.

7 ns pulse width, $\lambda = 532$ nm). The incident laser power was varied with a high-power variable beam splitter (CVI Corp) and measured with a power meter (Sciencetech Model 372). Transients were collected with an analyzing beam, digitized with a LeCroy Model 9310 digitizer, transferred to an IBM-compatible computer, and fit with the Marquardt nonlinear least-squares algorithm.¹⁵ Emission data were collected in situ using a fiber optic cable.

The triplet decays of both the $[\alpha\text{ZnM}, \beta\text{Fe}^{3+}(\text{N}_3^-)]$ and $[\alpha\text{Fe}^{3+}(\text{N}_3^-), \beta\text{ZnM}]$ hybrids in oxygen-free solution obey first-order kinetics for about 3 half-lives, independent of excitation power. In contrast, the triplet decay of $(\text{ZnM})\text{Hb}$ in anaerobic conditions shows a power dependence. At high excitation power, the triplet decay is only exponential after $t \approx 1$ ms. For $(\text{ZnP})\text{Hb}$, the early time multiphasic kinetics have been attributed to triplet-triplet energy-transfer processes within the Hb tetramer.²⁸ As the excitation power is lowered, the fraction of the nonexponential kinetics decreases and the triplet decay is nearly exponential at excitation powers of ~ 1 mJ/pulse. However, rather than reducing the S/N by lowering the power, it was satisfactory to collect data at high power, discard the data for $t \geq 1$ ms, and fit only the later time data.

Results

Optical Properties of [ZnM, FeP] Hybrids. We chose to study ZnM-substituted Hb because its optical properties are favorable for ET measurements. Figure 1 shows the optical spectra of $\text{HbA}_0(\text{CO})$, $(\text{ZnM})\text{Hb}$, and the $[\alpha\text{ZnM}, \beta\text{Fe}^{2+}(\text{CO})]$ hybrid; the $[\alpha\text{ZnM}, \beta\text{Fe}^{2+}(\text{CO})]$ and $[\alpha\text{Fe}^{2+}(\text{CO}), \beta\text{ZnM}]$ hybrids give nearly identical optical spectra. The Soret maximum for $(\text{ZnM})\text{Hb}$ ($\lambda_{\text{max}} = 414$ nm) is blue-shifted relative to that of $\text{HbA}_0(\text{CO})$ ($\lambda_{\text{max}} = 418$ nm) and $(\text{ZnP})\text{Hb}$ ($\lambda_{\text{max}} = 424$ nm).²⁹ The Soret maximum for all of the ZnP-substituted Hbs are much sharper and blue-shifted relative to deoxyHb ($\lambda_{\text{max}} = 430$ nm). The Soret band of the hybrid is dominated by the sharp peak of the ZnM chains ($\lambda_{\text{max}} = 414$ nm), but shows a shoulder for the $\text{Fe}^{2+}(\text{CO})$ chains on the long-wavelength edge. In fact, the spectrum of the hybrid can be simulated by averaging the spectra of $\text{Fe}^{2+}(\text{CO})\text{Hb}$ and $(\text{ZnM})\text{Hb}$ (circles in Figure 1).

The inset of Figure 1 shows the “ α - β ” region of the optical spectra. The spectrum of the $(\text{ZnM})\text{Hb}$ has two peaks at λ_{max}

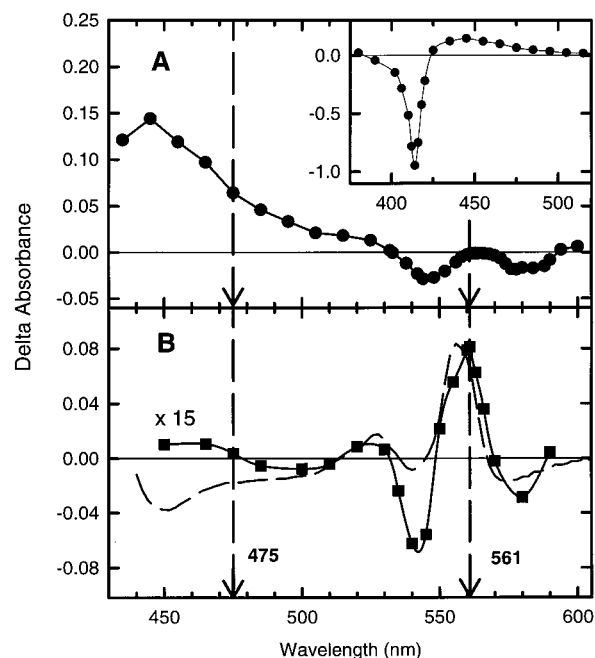


Figure 2. Kinetic difference spectra for the $[\alpha\text{ZnM}, \beta\text{Fe}^{3+}(\text{N}_3^-)]$ hybrid and b_5 . (A) $[\text{3D} - \text{G}]$ kinetic difference spectrum measured as the zero-time absorbance difference. (B) The $[\text{I} - \text{G}]$ kinetic difference spectrum measured as the time-resolved transient absorbance signal at $t = 10$ ms (■). The static difference spectrum of $[\text{Fe}^{2+}b_5 - \text{Fe}^{3+}b_5]$ (---). Conditions: 5 mM KPI, 5 mM NaN_3 , 0.05 mM IHP, pH 6.0, 20 °C.

$= 540$ and 580 nm with relative intensities of $R = \epsilon_{540}/\epsilon_{580} = 1.6$, which are slightly blue-shifted from the $\text{HbA}_0(\text{CO})$ peaks at $\lambda_{\text{max}} = 540$ and 570 nm with $R = 1.36$. The hybrid spectrum has peaks at $\lambda_{\text{max}} = 540$ and 580 nm with $R = 1.5$, which agrees with the calculated spectra.

The triplet-ground, $[\text{3D} - \text{G}]$, kinetic difference spectrum of the photoexcited $[\alpha\text{ZnM}, \beta\text{Fe}^{3+}(\text{N}_3^-)]$ hybrid has been measured as the zero-time absorbance difference following flash photolysis (Figure 2A); within experimental error, the spectrum of the $[\alpha\text{Fe}^{3+}(\text{N}_3^-), \beta\text{ZnM}]$ hybrid is identical. This figure shows the characteristic bleaching of the Soret absorbance ($\lambda_{\text{max}}^- = 414$ nm) (inset) and positive absorbance difference from 425 to 530 nm ($\lambda_{\text{max}}^+ = 445$ nm). The triplet kinetics were monitored at 475 nm because this wavelength is near an isosbestic point in the intermediate-ground, $[\text{I} - \text{G}]$ kinetic difference spectrum which is described below. Figure 2A also shows that there are three $[\text{3D} - \text{G}]$ isosbestic points at 530, 561, and 590 nm in the wavelength range of 450–600 nm.

The time course of the ET intermediate, **I**, can be followed by monitoring the transient absorbance signal at a $[\text{3D} - \text{G}]$ isosbestic point. The inset of Figure 3 shows that the signal for **I** persists at least 50 times longer than the signal for 3D and exhibits an absorbance maximum at $t \approx 2$ ms.³⁰ The $[\text{I} - \text{G}]$ kinetic difference spectrum has been obtained at $t = 10$ ms after the flash, when all of 3D is gone (Figure 2B). This spectrum shows a negative absorbance maximum at 540 nm and a positive absorbance maximum at 561 nm, a $[\text{3D} - \text{G}]$ isosbestic point. Figure 2B also shows the static $[\text{Fe}^{2+}b_5 - \text{Fe}^{3+}b_5]$ difference spectrum (dashed line). Comparison with the $[\text{I} - \text{G}]$ kinetic difference spectrum shows that the spectrum of **I** from 540 to 580 nm is dominated by the b_5 reduction, confirming that the triplet quenching occurs by photoinitiated ET. We chose to work with the ZnM-substituted proteins because the $[\text{3D} - \text{G}]$

(28) Zemel, H.; Hoffman, B. M. *J. Am. Chem. Soc.* **1981**, *103*, 1192–1201.

(29) Hoffman, B. M. *J. Am. Chem. Soc.* **1975**, *97*, 1688–1694.

(30) The progress of **I** cannot be adequately described by a single kinetic phase, and a detailed analysis is in progress.

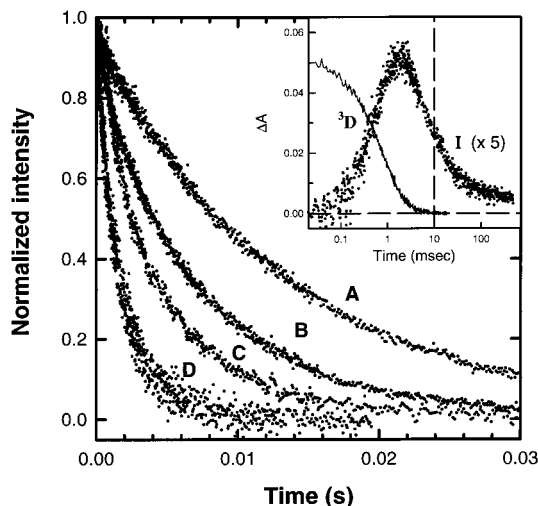


Figure 3. Normalized triplet decay curves for the titration of the [ZnM, $\text{Fe}^{3+}(\text{N}_3^-)$] hybrids and (ZnM)Hb with $\text{Fe}^{3+}b_5$. (A) 4 μM [αZnM , $\beta\text{Fe}^{3+}(\text{N}_3^-)$] hybrid without $\text{Fe}^{3+}b_5$; (B) 4 μM [$\alpha\text{Fe}^{3+}(\text{N}_3^-)$, βZnM] hybrid with [$\text{Fe}^{3+}b_5$] = 23 μM ; (C) 4 μM (ZnM)Hb with [$\text{Fe}^{3+}b_5$] = 22 μM ; (D) 4 μM [αZnM , $\beta\text{Fe}^{3+}(\text{N}_3^-)$] hybrid with [$\text{Fe}^{3+}b_5$] = 22 μM . Conditions: 5 mM KPi, 5 mM NaN_3 , 0.05 mM IHP, pH 6.0 for the hybrids and 10 mM KPi, 0.05 mM IHP, pH 6.0 for the (ZnM)Hb, all at 20 °C. Inset: Time courses of the triplet (^3D) recorded at 475 nm and the ET intermediate (I) plotted at 561 nm. The dotted line at $t = 10$ ms indicates the time slice recorded in Figure 2B. Conditions: 8.2 μM [αZnM , $\beta\text{Fe}^{3+}(\text{N}_3^-)$] hybrid and 47 μM b_5 ; 5 mM KPi, 5 mM NaN_3 , 0.05 mM IHP, pH 6.0, 20 °C.

isosbestic for the ZnP protein falls at 572 nm,³¹ near an isosbestic in the [I – G] difference spectrum.

Triplet Decay Kinetics of [ZnM, FeP] Hybrids and (ZnM)-Hb. Figure 3A shows the time-resolved triplet decay for the [αZnM , $\beta\text{Fe}^{3+}(\text{N}_3^-)$] hybrid in the absence of b_5 ; the trace for the βZn hybrid is indistinguishable. The decay traces for both hybrids are exponential with a rate constant of $k_{\text{hyb}}^{\text{d}} = 75 \pm 5 \text{ s}^{-1}$.³² When $\text{Fe}^{3+}b_5$ is added, the $^3\text{ZnM} \rightarrow \text{Fe}^{3+}b_5$ interprotein ET differentially decreases the triplet lifetime of both hybrids. For example, at a ca. 5-fold excess of $\text{Fe}^{3+}b_5$ the decay rate constant for the [$\alpha\text{Fe}^{3+}(\text{N}_3^-)$, βZnM] hybrid increases to $k_{\beta}^{\text{obs}} = 142 \text{ s}^{-1}$ (Figure 3B), while that of the [αZnM , $\beta\text{Fe}^{3+}(\text{N}_3^-)$] hybrid increases to $k_{\alpha}^{\text{obs}} = 566 \text{ s}^{-1}$ (Figure 3D). As a hybrid contains the ZnM photoprobe in only one chain type, either the α - or the β -chain, the quenching of a hybrid by $\text{Fe}^{3+}b_5$ is associated only with the reaction at that chain.

The triplet decay of the fully substituted (ZnM)Hb is exponential ($k^{\text{d}} = 59 \pm 6 \text{ s}^{-1}$), with the decays of the two chains not resolvable (not shown). In the presence of $\text{Fe}^{3+}b_5$, the triplet lifetime of (ZnM)Hb also decreases, with the trace lying between those of the hybrids for any given [$\text{Fe}^{3+}b_5$] (Figure 3C). Figure 4 shows that the (ZnM)Hb decay trace is *not* well-described by an exponential when b_5 is present, but rather it is well-fit by a biexponential function with equal contributions of the two components (rate constants, k_i^{obs} , $i = 1, 2$).

Binding of b_5 to [ZnM, FeP] Hybrids and (ZnM)Hb. To measure the binding of b_5 to hemoglobin, both the [αZnM , $\beta\text{Fe}^{3+}(\text{N}_3^-)$] hybrid and [$\alpha\text{Fe}^{3+}(\text{N}_3^-)$, βZnM] hybrid, as well as (ZnM)Hb, were titrated with $\text{Fe}^{3+}b_5$. The triplet decay traces of the hybrids remain exponential throughout the titration, while

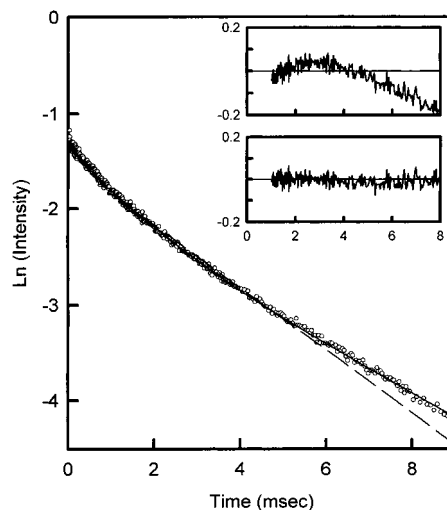
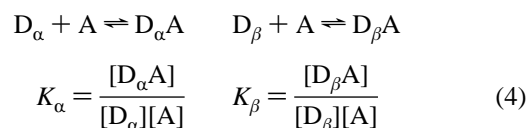


Figure 4. Semilog plot of the triplet decay of 4 μM (ZnM)Hb and 24 μM $\text{Fe}^{3+}b_5$ with exponential (—) and biexponential (---) decay fits. Insets: Residual plots for the exponential (upper) and biexponential (lower) fits. Conditions: 10 mM KPi, 0.05 mM IHP, pH 6.0, 20 °C.

those of the (ZnM)Hb remain biexponential with equal contributions of the two components. This behavior indicates that the exchange between the [Hb, b_5] complex and its components is fast ($k_{\text{off}} \gg k_{\text{obs}}$). Figure 5 shows the [$\text{Fe}^{3+}b_5$] dependence of the quenching constants ($\Delta k_i = k_i^{\text{obs}} - k_{\text{hyb}}^{\text{d}}$, $i = \alpha, \beta$) obtained from the titrations of the two hybrids (filled symbols), as well as those for the two quenching constants resolved from the biexponential fits to the decays of (ZnM)Hb (open symbols) at pH 6.0 and 7.0. Clearly, the two quenching constants derived from the biexponential fitting of the (ZnM)Hb decay traces correspond to those of the two hybrids; the larger of the two corresponds to the quenching constant of the αZn chain ($\Delta k_1 \leftrightarrow \Delta k_{\alpha}$) and the smaller to that of the βZn chain ($\Delta k_2 \leftrightarrow \Delta k_{\beta}$). This shows that the data from the hybrids and the (ZnM)Hb are consistent, and confirms that the two parallel quenching processes observed for (ZnM)Hb correspond to the reactions of the two types of chains with b_5 .

At pH 6.0, the quenching profile for the αZn chains (Figure 5A) shows appreciable curvature, confirming that ET at the αZn chain occurs within a bound complex rather than by a simple bimolecular quenching mechanism which would show a linear dependence on [b_5]. As seen by a comparison to a straight-line fit to the data for [b_5] $\leq 15 \mu\text{M}$, the quenching titration profile for the βZn chains (Figure 5B) also deviates from linearity at high [$\text{Fe}^{3+}b_5$], indicating that the ET quenching for the βZn chains also involves complex formation. However, the titration profile for the βZn chains shows less curvature than the titration profile for the αZn chains, suggesting that the binding is weaker for the βZn chains than for the αZn chains. The solid lines in Figure 5 are fits with a model now described.

The combined data of the hybrids and (ZnM)Hb are consistent with a model in which each monomer within the $\alpha_2\beta_2$ Hb tetramer *independently* binds a molecule of b_5 (A), where the macroscopic binding constant for the α -chains (D_{α}) is K_{α} and that for the β -chains (D_{β}) is K_{β} , according to eq 4. These two



equilibrium equations are linked by the mass balance equation

(31) Kuila, D.; Natan, M. J.; Rogers, P.; Gingrich, D. J.; Baxter, W. W.; Arnone, A.; Hoffman, B. M. *J. Am. Chem. Soc.* **1991**, *113*, 6520–6526.

(32) The rate constant k^{d} is the sum of the intrinsic decay rate constant, $k^{\text{d}} \approx 59 \pm 6 \text{ s}^{-1}$, as measured for (ZnM)Hb and the intersubunit $\alpha_1\text{-}\beta_2$ ET rate constant, $k_{\text{int}} \approx 16 \text{ s}^{-1}$.

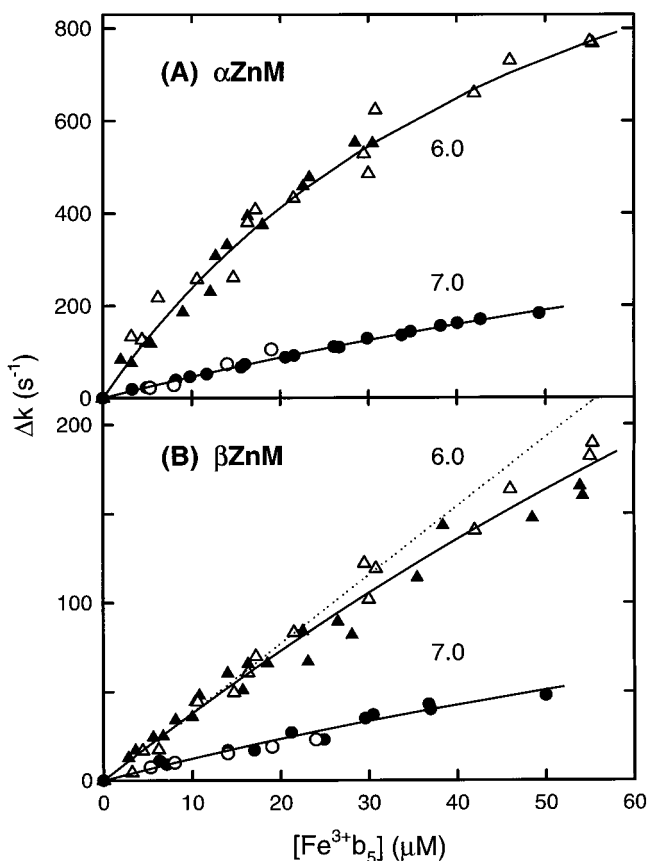


Figure 5. Triplet quenching of (ZnM)Hb by $\text{Fe}^{3+}b_5$ at pH 6.0 and pH 7.0. Titration profiles for the αZnM chains (A) and the βZnM -chains (B) in the $[\text{ZnM}, \text{Fe}^{3+}(\text{N}_3^-)]$ Hb hybrids and in (ZnM)Hb. At each pH, the hybrid data are shown by the filled symbols and the two quenching rate constants obtained from the biexponential fitting of (ZnM)Hb are shown by the open symbols ($\Delta k_1 \leftrightarrow \Delta k_\alpha$; $\Delta k_2 \leftrightarrow \Delta k_\beta$). The solid lines are fits to the binding model described in the text with the fitting parameters summarized in Table 1. The dotted line in panel B is obtained by fitting the quenching data ($[\text{Fe}^{3+}b_5] \leq 15 \mu\text{M}$) to a simple bimolecular quenching model. Conditions: 5 mM KPi, 5 mM NaN₃, 0.05 mM IHP for the hybrids and 10 mM KPi, 0.05 mM IHP for (ZnM)-Hb, at 20 °C.

for b_5 (eq 5). The concentration of b_5 which is bound to the

$$[\text{A}]_0 = [\text{A}] + [\text{D}_\alpha\text{A}] + [\text{D}_\beta\text{A}] \quad (5)$$

αZn chains, $[\text{D}_\alpha\text{A}]$, can be calculated by solving a cubic equation for $[\text{D}_\alpha\text{A}]$ that can be generated from eqs 4 and 5,

$$c_1[\text{D}_\alpha\text{A}] + c_2[\text{D}_\alpha\text{A}]^2 + c_3[\text{D}_\alpha\text{A}]^3 + c_4 = 0 \quad (6)$$

where the coefficients are functions of the initial concentration of b_5 ($[\text{A}]_0$), the initial concentration of the Hb subunits ($[\text{D}_\alpha]_0 = [\text{D}_\beta]_0 \equiv [\text{D}]_0$), and the ratio of the binding constants (eq 7).

$$m = K_\alpha/K_\beta$$

$$c_1 = K_\alpha(1 - m)$$

$$c_2 = K_\alpha(2m[\text{D}]_0 + m[\text{A}]_0 - [\text{A}]_0) + m - 1$$

$$c_3 = K_\alpha([\text{D}]_0[\text{A}]_0 - [\text{D}]_0^2 - m[\text{D}]_0^2 - 2m[\text{D}]_0[\text{A}]_0) - m[\text{D}]_0$$

$$c_4 = K_\alpha m[\text{D}]_0^2[\text{A}]_0 \quad (7)$$

The solution of eq 6 for $[\text{D}_\alpha\text{A}]$ can be used to obtain the concentration of b_5 which is bound to the βZn chains, $[\text{D}_\beta\text{A}]$, and, most usefully, the concentration of b_5 that remains unbound, $[\text{A}]$.

$$[\text{A}] = [\text{A}]_0 - \left(\frac{(1+m)[\text{D}]_0 + (1-m)[\text{D}_\alpha\text{A}]}{m[\text{D}]_0 + (1-m)[\text{D}_\alpha\text{A}]} \right) [\text{D}_\alpha\text{A}] \quad (8)$$

The fractions of the two chain types that reside within a complex (f_α, f_β) are then given by eq 9.

$$f_\alpha = \frac{[\text{D}_\alpha\text{A}]}{[\text{D}]_0} = \frac{K_\alpha[\text{A}]}{1 + K_\alpha[\text{A}]} \quad f_\beta = \frac{[\text{D}_\beta\text{A}]}{[\text{D}]_0} = \frac{K_\beta[\text{A}]}{1 + K_\beta[\text{A}]} \quad (9)$$

In the hybrids, only one chain type has a ZnM photoprobe, while the other chain has an unreactive Fe^{3+} heme. In the fast-exchange limit that describes these experiments ($k_{\text{off}} \gg k_{\text{obs}}$), the triplet decay traces for the hybrids are described by the exponential functions (eq 10). At any point in a titration, the

$$\begin{aligned} \Delta A_\alpha &= A_0 e^{-k_\alpha^{\text{obs}} t} & \Delta A_\beta &= A_0 e^{-k_\beta^{\text{obs}} t} \\ k_\alpha^{\text{obs}} &= k_\alpha^d + \Delta k_\alpha & k_\beta^{\text{obs}} &= k_\beta^d + \Delta k_\beta \end{aligned} \quad (10)$$

measured quenching for each Zn-substituted chain ($\Delta k_\alpha, \Delta k_\beta$) is the product of the ET rate constant for that chain (k_α, k_β) and the fraction of that chain with a bound b_5 (f_α, f_β) (eq 11).

$$\Delta k_\alpha = k_\alpha f_\alpha \quad \Delta k_\beta = k_\beta f_\beta \quad (11)$$

For (ZnM)Hb, both chain types contain the ZnM photoprobe and the observed triplet decays are described by the biexponential function (eq 12).

$$\Delta A = A_0 \left(\frac{e^{-k_\alpha^{\text{obs}} t} + e^{-k_\beta^{\text{obs}} t}}{2} \right) \quad (12)$$

The solid lines in Figure 5 are the fits to the binding model; the binding constants (K_α, K_β) and the ET rate constants (k_α, k_β) are summarized in Table 1. Cytochrome b_5 binds with comparable strength to the two types of chains, with binding at the α -chain being ~ 4 -fold tighter ($K_\alpha = 1.9 \times 10^4 \text{ M}^{-1}$; $K_\beta = 4.9 \times 10^3 \text{ M}^{-1}$ at pH 6.0), while the rate constant for the ET reaction with $\text{Fe}^{3+}b_5$ is ~ 2 -fold greater for the αZnM chain than for the βZnM chain ($k_\alpha = 1500 \text{ s}^{-1}$; $k_\beta = 850 \text{ s}^{-1}$). From spectrophotometric measurements, Mauk and Mauk report a single binding constant of comparable value, $K = (9 \pm 3) \times 10^3 \text{ M}^{-1}$, under similar conditions ($\mu = 12 \text{ mM}$, pH 6.2);⁵ the lack of resolution of a ca. 4-fold difference in binding constants is not surprising.³³

pH Dependence. Figure 5 also shows the titration profiles for the αZnM chains (A) and the βZnM chains (B) in the $[\text{ZnM}, \text{Fe}^{3+}(\text{N}_3^-)]$ Hb hybrids (filled symbols) and in (ZnM)Hb (open symbols) at pH 7.0. The solid lines are fits to the model described above; the resulting binding and rate constants are given in Table 1. The binding affinity of the β -chain is essentially unchanged, while the ET rate constant decreases ~ 4 -fold, from $k_\beta = 850 \text{ s}^{-1}$ to $k_\beta = 230 \text{ s}^{-1}$, as the pH increases from 6.0 to 7.0. The binding of b_5 to the α -chains weakens, with an approximately 3-fold decrease in the binding constant, as the pH increases from 6.0 to 7.0, with the result that at pH 7.0 the binding affinity for the α -chains is the same as for the

(33) Given the agreement with Mauk and Mauk, we are unable to account for a report that the binding constant is more than an order of magnitude less.⁷

Table 1. Association Constants (K_A) and ET Rate Constants (k) of the $[\alpha\text{ZnM}, \beta\text{Fe}^{3+}(\text{N}_3^-)]$ Hybrid: $\text{Fe}^{3+}b_5$ and the $[\alpha\text{Fe}^{3+}(\text{N}_3^-), \beta\text{ZnM}]$ Hybrid: $\text{Fe}^{3+}b_5$ Complexes

protein	pH 6.0		pH 7.0	
	$K_A (\times 10^3 \text{ M}^{-1})$	$k (\text{s}^{-1})$	$K_A (\times 10^3 \text{ M}^{-1})$	$k (\text{s}^{-1})$
$[\alpha\text{ZnM}, \beta\text{Fe}^{3+}(\text{N}_3^-)]$	19 ± 2	1500 ± 80	5.9 ± 0.8	840 ± 90
$[\alpha\text{Fe}^{3+}(\text{N}_3^-), \beta\text{ZnM}]$	4.9 ± 3.6	850 ± 520	5.9 ± 2.6	230 ± 80
sperm whale Mb ¹⁵	<3	$\geq 4.6 \times 10^4$	<3	≥ 3600
horse heart Mb ¹⁶	0.75 ± 0.1	$(5.9 \pm 0.5) \times 10^4$	<2	$\geq (3.1 \pm 0.5) \times 10^3$
bovine Mb ⁴³	$>100^a$			

^a pH = 5.6.

β -chains. Table 1 shows that the reactivity for the αZnM chains also decreases, but by ~ 2 -fold (from $k_\alpha = 1500 \text{ s}^{-1}$ at pH 6.0 to 840 s^{-1} at pH 7.0).

Discussion

We have used the triplet quenching of the $[\text{ZnM}, \text{Fe}^{3+}(\text{N}_3^-)]$ Hb hybrids and $(\text{ZnM})\text{Hb}$ by $\text{Fe}^{3+}b_5$ to measure the binding affinity and intracomplex ET rate constants for the reaction of $\text{Fe}^{3+}b_5$ with the subunits of Hb. Thermodynamic studies show that Zn-substituted Hb adopts the T-state,^{34,35} and flash photolysis CO-rebinding studies show that the mixed-metal Hb hybrids are in the T-state as well.²³ Use of the hybrids allowed us to separately characterize the interactions of b_5 with the α -chains and the β -chains within the T-state $\alpha_2\beta_2$ tetramer. The results for the hybrids are completely consistent with those for $(\text{ZnM})\text{Hb}$, with the biphasic kinetics observed for $(\text{ZnM})\text{Hb}$ resulting from independent reactions of $\text{Fe}^{3+}b_5$ at the two chain types.

The triplet quenching titration curves have been fit with a model in which each chain of a Hb tetramer independently binds and reacts with b_5 , but with different affinities and different intracomplex ET rate constants for the α - and β -chains. At pH 6.0, the α -chain affinity for b_5 is ~ 4 -fold larger than that of the β -chains ($K_\alpha = 1.9 \times 10^4 \text{ M}^{-1}$; $K_\beta = 4.9 \times 10^3 \text{ M}^{-1}$), whereas the ET rate constant for the α -chains is ~ 2 -fold greater than that for the β -chains ($k_\alpha = 1500 \text{ s}^{-1}$; $k_\beta = 850 \text{ s}^{-1}$). These results are consistent with the ET rate constants that McLendon and co-workers reported for the triplet quenching of ZnHb by $\text{Fe}^{3+}b_5$ ($k_1 = 2700 \text{ s}^{-1}$ and $k_2 = 310 \text{ s}^{-1}$; 1 mM KPi, pH 6.2). On the basis of our results, we can identify their k_1 with the reaction at the α -chains and k_2 with the reaction at the β -chains. It is interesting to speculate that the weak binding and rapid association/dissociation rate constants are useful for reaction in the red cell, where the concentration of Hb is high and most of the Hb is *not* oxidized.

Prior reports of the ET reactivity differences of the Hb chains have been inconsistent. Reactions with inorganic complexes have shown that oxidation of Hb depends on the quaternary state and that the ET mechanism depends on the chain type. Mansouri and Winterhalter report that upon treatment of R-state oxyHb with $\text{K}_3\text{Fe}(\text{CN})_6$ the rate of oxidation of the α -chain is ~ 10 -fold greater than that of the β -chain as determined by absorption spectroscopy.³⁶ In contrast, Perrella and co-workers show that by cryogenic techniques the rate of oxidation of the β -chains of T-state deoxyHb by $\text{K}_3\text{Fe}(\text{CN})_6$ is 4-times faster than that of the α -chain.³⁷ The oxidation of a mixture of deoxy-

and oxyHb by metal chelates also shows differences in the oxidation reactions of the chains. Saltman has demonstrated that the reaction of $\text{Cu}(\text{II})$ -bis(bathocuproine) with Hb involves the site specific binding of the metal chelate at Cys93 on the β -chain; however, the reaction with the α -chain occurs through an outer-sphere mechanism.³⁸

Of more direct relation to the present work, differences in ET reactivity of the Hb chains have also been reported for the enzymatic reduction of Fe^{3+}Hb by the $b_5\text{R}$ and b_5 system. In contrast to our results, work by Tomoda and co-workers using isoelectric focusing gels and absorption spectra showed that the β -chains are more reactive than the α -chains.³⁹ However, this study was at higher ionic strength (0.05 M Bis-Tris, 0.140 M NaCl, pH 7), and the separation procedure was performed at 4 °C, during which the charges may have redistributed. Thus, an advantage to our metal-substitution method is that we separately monitor the redox reactions at each chain type while they occur.

Where Does b_5 Bind? Early computer graphics modeling of the $[\text{Fe}^{3+}\text{Hb}(\text{horse}), \text{Fe}^{3+}b_5(\text{bovine})]$ complex identified a possible docking site on each subunit.¹⁷ Complexes of the individual subunits and b_5 were generated by the manual manipulation of the protein structures to optimally align the basic residues of each chain with the acidic residues on b_5 . The conclusion was that, for each subunit, the ϵ -amino side chains of a set of Lys residues on the E-helix and the FG-corner interact with the carboxylate side chains of residues from helix III (Glu 48, Glu 44, and Glu 43) and helix IV (Asp 60) of b_5 .⁴⁰ The locations of the relevant surface Lys residues of Hb are shown in Figure 6A. However, because the sequences of the α - and β -chains differ, b_5 forms four electrostatic contacts with a β -chain (Lys 59 (E3), Lys 61 (E5), Lys 65 (E9), and Lys 95 (FG2)), but only three with an α -chain (Lys 56 (E5), Lys 60 (E9), and Lys 90 (FG2)). In addition to these contacts, Lys 61 (E10) of the α -chain and Lys 66 (E10) of the β -chain bridge the heme propionate of that subunit with the heme propionate of b_5 . Our experimental observation that the two chains have similar binding affinities is consistent with there being approximately the same number and type of contacts between each subunit and b_5 .

The structural model for the $[\text{Hb}, b_5]$ complex has received some support from experiments using naturally occurring charge-reversal Hb variants,¹⁸ namely, Hb I Toulouse ($\beta 66 \text{ KE}$), Hb N Baltimore ($\beta 95 \text{ KE}$), and Hb I Philadelphia ($\alpha 16 \text{ KE}$). The thermal ET between b_5 and the iron-containing β -chain variants was remarkably different from that of native HbA_o, indicating that the Lys residues on the β -chain at positions 66 (E10) and 95 (FG2) are important to the reaction with b_5 . However, the kinetic behavior of the α -chain variant was

(34) Huang, Y.; Yonetani, T.; Tsuneshige, A.; Hoffman, B. M.; Ackers, G. K. *Proc. Natl. Acad. Sci. U.S.A.* **1996**, *93*, 4425–4430.

(35) Huang, Y.; Doyle, M. L.; Ackers, G. K. *Biophys. J.* **1996**, *71*, 2094–2105.

(36) Mansouri, A.; Winterhalter, K. H. *Biochemistry* **1973**, *12*, 4946–4949.

(37) Perrella, M.; Shrager, R. I.; Ripamonti, M.; Manfredi, G.; Berger, R. L.; Rossi-Bernardi, L. *Biochemistry* **1993**, *32*, 5233–5238.

(38) Eguchi, L. A.; Saltman, P. *Inorg. Chem.* **1987**, *26*, 3669–3672.

(39) Tomoda, A.; Yubisui, T.; Tsuji, A.; Yoneyama, Y. *J. Biol. Chem.* **1979**, *254*, 3119–3123.

(40) Durlay, R. C. E.; Mathews, F. S. *Acta Crystallogr.* **1996**, *D52*, 65–76.

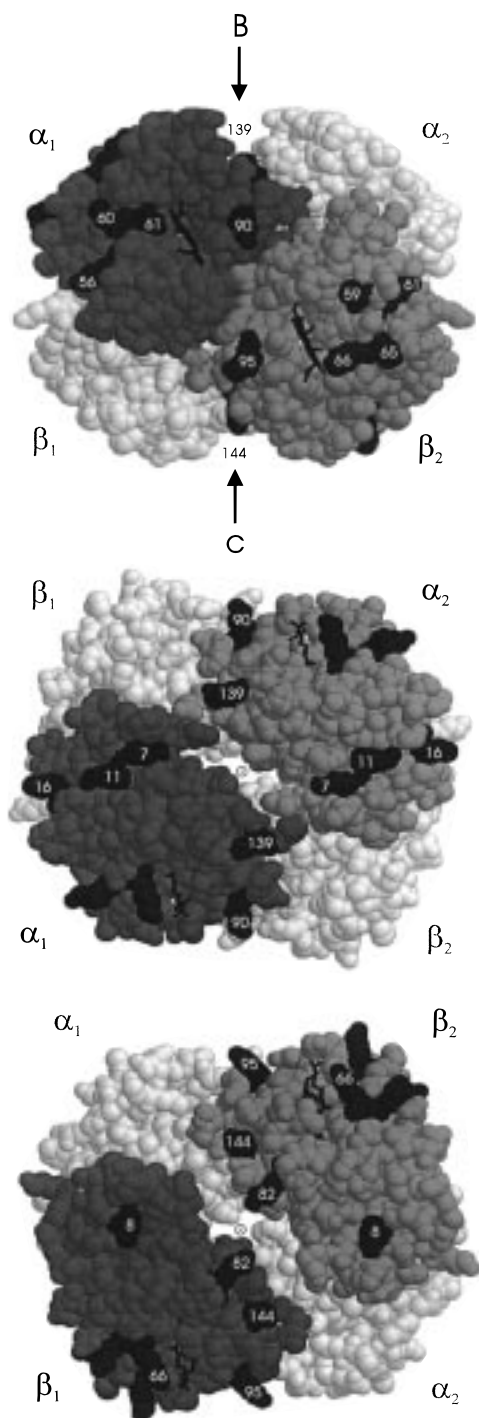


Figure 6. Space-filling representations of Hb with the Lys residues discussed in the text shown in black. The hemes are shown in stick representation. (A, top) View of the α_1 - and β_2 -chains with the Lys residues that form the b_5 binding site as indicated by the computer modeling labeled in white. The arrows indicate the viewpoints for (B) and (C) with α Lys 139 and β Lys 144 labeled as reference points. (B, middle) View of the α_1 - and α_2 -chains with the Lys residues at positions 7 (A5), 11 (A9), and 139 (HC1) shown as proposed contacts for an $\alpha_1\alpha_2$ -site. Lys 90 is labeled as a reference point for view (A). Lys 16 (A14) is the mutation site of the Hb I Philadelphia (α 16 KE) variant. (C, bottom) View of the β_1 - and β_2 -chains with the Lys residues at positions 8 (A5), 82 (EF6), and 144 (HC1) shown as proposed contacts for a $\beta_1\beta_2$ -site. The Lys residues at positions 66 (E10) and 95 (FG2) are the mutation sites of the Hb I Toulouse (β 66 KE) and Hb N Baltimore (β 95 KE) variants, respectively. These figures were generated from the PDB file 3HHB⁴⁵ using RasMol.

identical to that of native HbA₀, indicating that Lys 16 (A14) on the α -chain is not involved in the interaction with b_5 .

While the above interpretation is quite plausible, our kinetic model is not distinguishable from one in which both α -chains undergo ET from b_5 bound at a single site that is symmetrically placed between the two α -chains ($\alpha_1\alpha_2$ -site), and/or that both β -chains react with b_5 bound independently at a site between the two β -chains ($\beta_1\beta_2$ -site). In this model, reduction of two α - or β -chains would necessarily occur sequentially rather than in parallel, but the b_5 binding is not tight enough to detect such a difference kinetically. Examination of the Hb tetramer surface suggests possible locations for such binding sites. An $\alpha_1\alpha_2$ -site might be defined by the Lys residues at positions 7 (A5), 11 (A9), and 139 (HC1) on one α -chain and the Lys residue at 139 (HC1) on the other α -chain as shown in Figure 6B. Such a proposed binding site is consistent with the results of the variant study, in that Lys 16 (A14) of the α -chain is not involved with b_5 binding.¹⁸ Such a site would be influenced by the T-R conversion.⁷ A complementary $\beta_1\beta_2$ -site situated near the IHP binding site⁴¹ could involve Lys residues at positions 8 (A5), 82 (EF6), and 144 (HC1) on the two β -chains as indicated in Figure 6C. However, in the present study IHP is bound to Hb which should prevent the binding of b_5 at such a site. Furthermore, this proposal is inconsistent with the variant study, because this site appears to exclude the involvement of Lys residues at positions 66 and 95.¹⁸ Therefore, while b_5 might react with the α -chains at an $\alpha_1\alpha_2$ -site, it seems likely that the reaction with the β -chains involves b_5 binding at independent sites on each β -chain, as proposed by the computer graphics modeling.⁴²

Comparison of [Hb, b_5] and [Mb, b_5] Complexes. Table 1 compares the binding affinities and ET rate constants for the reaction of bovine b_5 with the Hb chains and with homologous and heterologous Mbs. The binding of bovine b_5 to its homologous partner (i.e., bovine Mb)⁴³ is tighter than binding to heterologous Mb partners (e.g., sperm whale or horse heart Mb),^{15,16} while binding to human Hb is of intermediate strength. As there are fewer basic residues in either Hb chain than in Mb (11 Lys residues in each Hb chain vs 19 Lys residues in Mb), the differences in affinity of b_5 for Hb and Mb likely reflect the surface arrangement of basic residues rather than just the number of charged residues. Interestingly, the nature of the docking sites leads to higher reactivity (k) in the [Mb, b_5] complexes relative to the [Hb, b_5] complexes.^{15,16} Future work will compare the present data for a heterologous [Hb, b_5] complex with those for the homologous complex of human b_5 ⁴⁴ and Hb.

Acknowledgment. This research has been supported by NIH Grants HL13531 and HL 51084.

JA982009V

(41) Arnone, A.; Perutz, M. F. *Nature* **1974**, *249*, 34–36.

(42) The result that $K_\alpha \neq K_\beta$ requires a kinetic model such as the two just described, in which the α - and β -chains undergo ET with b_5 bound at different surface sites. However, if the measured 4-fold difference in the binding constants at pH 6 is not significant, one might further consider a model in which there is only one type of binding site poised between the two chains. Such alternative binding sites have been considered, and experiments to further examine the relative binding constants are being developed.

(43) Livingston, D. J.; McLachlan, S. J.; La Mar, G. N.; Brown, W. D. *J. Biol. Chem.* **1985**, *260*, 15699–15707.

(44) Lloyd, E.; Ferrer, J. C.; Funk, W. D.; Mauk, M. R.; Mauk, A. G. *Biochemistry* **1994**, *33*, 11432–11437.

(45) Fermi, G.; Perutz, M. F.; Shaanan, B.; Fourme, R. *J. Mol. Biol.* **1984**, *175*, 159–174.